Key factors affecting prediction of seismic pore water pressures in silty sands based on damage parameter

- PORCINO D.D., Tomasello G., Diano V. (2018). Key factors affecting prediction of seismic pore water pressures in silty sands based on damage parameter. BULLETIN OF EARTHQUAKE ENGINEERING, (16):5801–5819, doi: 10.1007/s10518-018-0411-z

Key Factors Affecting Prediction of Seismic Pore Water Pressures In Silty Sands Based on Damage Parameter

Daniela D. PORCINO[1], Giuseppe TOMASELLO[2] & Valentina DIANO[3]

[1] *Associate Professor in Geotechnical Engineering, University "Mediterranea" of Reggio Calabria (Italy)*

[2] *Research Assistant, University "Mediterranea" of Reggio Calabria (Italy)*

[3] *Doctor of Philosophy in Civil, Environmental and Safety Engineering, University "Mediterranea" of Reggio Calabria (Italy)*

Corresponding author: Daniela D. Porcino daniela.porcino@unirc.it

Abstract

The paper provides insight into factors affecting the prediction of seismic pore-water pressure build up in clean sands and sand-silt mixtures for modeling purposes. Laboratory pore pressure measurements were conducted using stress-controlled undrained cyclic simple shear (CSS) tests carried out on both reconstituted and undisturbed specimens of silty sands under different initial conditions (density state, effective vertical stress, initial fabric and fines content). Test results were interpreted by using a damage concept-based model which is actually implemented for clean sands in non-linear time domain site response analysis codes. In the present work, such a model was properly modified for sands having fines contents higher than 35%. The general applicability of the modified procedure for predicting pore water pressure response of silty sands under irregular shear stress loading using data from stress-controlled *CSS* tests was also verified and all factors affecting calibration parameters of the model were throughly analyzed.

Keywords: Pore water pressure; earthquake; silty sands; damage-based model; cyclic simple shear tests.

1. Introduction

The simultaneous generation, dissipation, and redistribution of excess pore pressures within the layers of a soil deposit can significantly alter the stiffness and seismic response of the deposits. The importance of predicting pore water pressure induced by seismic events has been well recognized and the features of pore pressure generation for clean sands and silty sands have been extensively studied based on laboratory tests (Ishihara et al. 1976; Seed et al. 1978; Chang et al. 1981; Hazirbaba 2005; Derakhshandi et al. 2008; Dash and Sitharam 2009; Belkhatir et al. 2014; Konstadinou and Georgiannau 2014; Porcino and Diano 2016) and results of field measurements (Matasovic and Vucetic 1993; Chang 2002; Hazirbaba and Rathje 2004; Rathje et al. 2005; Chang et al. 2007).

Pore pressure generation models can generally be categorized into stress-based, strain-based, and energy-based models; whereas initial models for sands were primarily based on the results of cyclic stress-controlled tests (Lee and Albaisa 1974; Seed et al. 1975; Booker et al. 1976; Polito et al. 2008; Bazier et al. 2011), other research demonstrated improved correlation with the level of shear strain (Youd 1972; Martin et al. 1975; Mulilis et al. 1977; Dobry et al. 1985; Byrne 1991; Derakhshandi et al. 2008; Cetin and Bilge 2012) or the energy dissipated within the soil deposit (Berrill and Davis 1985; Figueroa et al. 1994; Green et al. 2000; Davis and Berrill 2001; Green 2001; Hashash et al. 2010; Polito et al. 2013). Stress-controlled tests apply uniform shear stresses and measure incremental build-up of pore pressure with the increase in the number of loading cycles. In the 1970s, Seed et al. (1975) developed an empirical model for predicting residual excess pore pressure ratio ($R_{u,res}$), which is defined as the ratio of the residual excess pore pressure to the initial effective vertical stress (σ'_{vo}) acting on the soil ($R_{u,res}=\Delta u/\sigma'_{vo}$). $R_{u,res}$ is a function of the cycle ratio, which is the ratio of the number of applied uniform cycles of loading (N) to the number of cycles required to cause liquefaction in the soil (N_f), and of an empirically determined parameter (β). Later, Booker et al. (1976) proposed an alternative, somewhat simplified version of this equation:

$$\mathrm{R_{u,res}} = \frac{2}{\pi} \cdot \arcsin\left(\frac{N}{\mathrm{N_f}}\right)^{1/2\beta} \tag{1}$$

A value of β=0.7 is recommended by Booker et al. (1976) for clean sands. Since the equations are identical in shape, both will be denoted as Seed model in this paper.

Based upon the results of approximately 150 cyclic triaxial (CTX) tests carried out on moist-tamped reconstituted specimens of sand with different non-plastic fines contents, a correlation relating β to relative density (D_r), cyclic stress ratio (CSR) and fines content (FC) was proposed by Polito et al. (2008) for sands with non-plastic fines, expressed as:

$$\beta = c_1 \cdot FC + c_2 \cdot D_r + c_3 \cdot CSR + c_4 \tag{2}$$

where FC and D_r are expressed as a percentage, CSR is the cyclic shear stress ratio imposed in CTX loading, and c_1, c_2, c_3, and c_4 are regression constants (dimensionless). For FC<35% regression coefficients determined by Polito et al. (2008) resulted: c_1=0.01166; c_2=0.007397; c_3=0.01034; and c_4=0.5058. On the other hand, for FC≥35% the regression coefficients were: c_1=0.002149; c_2=−0.0009398; c_3=1.667; and c_4=0.4285. Despite its simple form, the application of the relationship (1) is difficult as it requires that the earthquake motion be converted into an equivalent number of uniform loading cycles. Recently, there has been a development and application of the stress-based model based on damage parameter which uses the accumulated stress measurements from stress-controlled tests for predicting pore water pressure of sandy soils (Park and Ahn 2013; Park et al. 2015). The damage concept initially proposed by Finn and Bhatia (1982) is essentially a variable which contains parameters defining the strain and/or stress history, and can uniquely relate to build-up of pore pressure for a given soil (Ivši´c 2006). It is worth mentioning what is the main advantage of the model: since “damage” is an incremental parameter which increases with each time step, the model is suitable for use in incremental coupled (or uncoupled) effective stress dynamic analyses (Chiaradonna et al. 2015). Furthermore, the model can very easily be applied since all the input parameters can be selected from regular conventional cyclic stress or strain-controlled tests. Following the approach proposed by Park et al. (2015), the damage parameter relates the accumulated stress to residual pore pressure. The stress based damage parameter is defined as follows:

$$D = (\eta / CSR) \cdot (CSR - CSR_t)^{\alpha} \tag{3}$$

where CSR = shear stress ratio (shear stress normalized to initial effective vertical stress), CSR_t is the threshold shear stress ratio, separating conditions according to whether pore pressure rise can or cannot occur, and α is a curve fitting parameter. Threshold stress-strain level is a parameter with a clear physical meaning (e.g. Dobry et al. 1982;

Burghignoli et al. 1991; Vucetic 1994; Sagaseta 1995) and both laboratory and in situ testing results reflected a threshold strain (Hazirbaba and Rathje 2004).

An alternative to the stress history of the sample is the length of the stress path (η). This variable was defined as: $\eta = \int \frac{|d\tau|}{\sigma'_{vo}}$, where τ is the shear stress induced by seismic motion in the time domain. In particular, for a uniform regular loading history, η can be re-written as: $\eta = 4\ N\ CSR$. The relationship between the pore pressure ratio and the damage parameter was defined as the best fitting function through the available laboratory results. Traditionally, for clean sands or sands with low fines contents, the following modified equation based on the model proposed by Seed et al. (1975) is adopted (Park and Ahn 2013):

$$\mathrm{R_{u,res}} = \frac{2}{\pi} \cdot \arcsin\left(\frac{\mathrm{D}}{\mathrm{D_f}}\right)^{1/2\beta} \tag{4}$$

where D_f is the value of damage parameter at the onset of liquefaction and it is defined for a uniform cyclic stress history as follows:

$$D_f = 4 \cdot N_f \cdot (CSR - CSR_t)^{\alpha} \tag{5}$$

In the present work, the procedure followed for the determination of the model's parameters is described below:

1) The adopted equation of the laboratory liquefaction curve is the following:

$$\left(\frac{\mathrm{CSR - CSR_t}}{\mathrm{CSR_{ref} - CSR_t}}\right)^{\alpha} = \left(\frac{\mathrm{N_{ref}}}{\mathrm{N}}\right) \tag{6}$$

where CSR_{ref} is the *CSR* value at a reference number of loading cycles, and the parameter α describes the steepness of the (N, CSR) curve.

The selection of (N_{ref}, CSR_{ref}) point can be arbitrary; in the present study, for simplicity, N_{ref}= 15 was assumed as a reference number of cycles.

2) In the absence of specific tests, a value of the first parameter "CSR_t", corresponding to a high number of loading cycles (i.e. N=500) of the *CSR-N* curve was assumed. The appropriateness of this selection procedure was validated and it was verified that such a

value can be reasonably assumed for practical applications, providing a value close to an "optimum" CSR_t, i.e. corresponding to the lowest coefficient of variation (*COV*) of α, according to the procedure suggested Park et al. (2015) . However, in the present study it was verified that this optimum CSR_t value does not always exist and, in these cases, an alternative simple method has to be adopted.

3) the second parameter "α" was determined by Eq. (6) by fitting the curve to experimental data using "Least Square Method".

In case of silty sands with higher percentage of fines, Eq. (4) has some limitations and should be properly revised, as will be discussed in the following sections.

This paper sheds light on the key factors controlling the induced cyclic pore water pressure generation of clean sands and silty sands for modeling purposes. Therefore, a large database of high quality stress-controlled cyclic simple shear (*CSS*) tests were conducted on several materials: four clean sands, non-plastic sand-silt mixtures (*FC* ranging from 0 to 40%) and undisturbed samples of low plasticity sandy silts (*FC* from 40 to 70%). The pore water pressures were expressed directly as a monotonically increasing function of the damage parameter to verify the applicability of the model for a wide range of soils, and to derive representative calibration parameters, which encompass the effect of cyclic stress ratios (*CSR*), relative density (D_r), initial fabrics and fines content. Finally, for sands with a high percentage of fines (*FC*>35%), a modified relationship of the model was herein proposed based on *CSS* tests performed on undisturbed samples of sandy silts.

2. Materials and test program

Stress-controlled cyclic simple shear tests were performed on three clean silica sands with different grain-size features, namely: Ticino sand (*TS*), Ticino fine sand (*TSF*), Emilia sand (*ES*). In the present study, various reconstitution methods resulting in different fabrics and a wide variety of densities were adopted for preparing sand specimens, namely water sedimentation (*WS*), dry air deposition (*AP*) and moist tamping (*M*T).

Specimens of silty sands (0≤*FC*≤40%) were prepared by mixing Ticino sand with different percentage of non-plastic fines and moist-tamped at a prefixed (global) void ratio (e_0=0.68). The maximum and minimum void ratios of soils were determined in accordance with ASTM D 4254-00 and ASTM D 4253-00, respectively.

In order to investigate the excess pore water pressure build-up of sands with high fines contents (40≤*FC*≤70%), good-quality undisturbed samples of low plasticity sands+silt recovered by an Ostenberg sampler from a site in the Emilia Romagna region after the 2012 earthquake in Italy (Tonni et al. 2015; Porcino and Diano 2016) were tested in cyclic *SS* apparatus. Physical properties of all tested sandy and silty soils are reported in Table 1, while Figure 1 reports their grain size-distribution curves.

Table 1 – Main properties of tested materials.

Soil type	FC [%]	D_{50} [mm]	D_{10} [mm]	C_u	G_s	e_{min}	e_{max}
Gioia Tauro sand (GTS)	0.66	2.00	1.00	2.15	2.69	0.45	0.69
Ticino sand (TS)	0.43	0.56	0.42	1.45	2.66	0.56	0.91
Emilia sand (ES)	4.15	0.32	0.12	2.80	2.70	0.54	0.93
Ticino fine sand (TSF)	2.40	0.18	0.11	1.91	2.69	0.61	0.98
Emilia silty sand (ESS)	40	0.096	0.005	24.00	2.77	-	-
Emilia sandy silt (ESs)	70	0.034	0.002	17.00	2.77	-	-
Silt	100	0.025	0.004	7.82	2.72	-	0.80

Testing was performed using a modified cyclic simple shear *NGI* (Norwegian Geotechnical Institute) apparatus (Porcino et al. 2006). The specimens are 80 mm in diameter and 20 mm in height, and they are laterally confined by a reinforced rubber membrane, capable of assuring conditions of zero horizontal deformation (K_0 consolidation). In this type of apparatus the undrained tests are of the constant volume type: the changes in vertical stress to maintain constant volume are equivalent to the changes in pore-water pressure in the corresponding undrained test (Finn 1985; Dyvik et al. 1987). Thus, membrane compliance problems which could otherwise affect the pore pressures measurements during undrained tests are avoided.

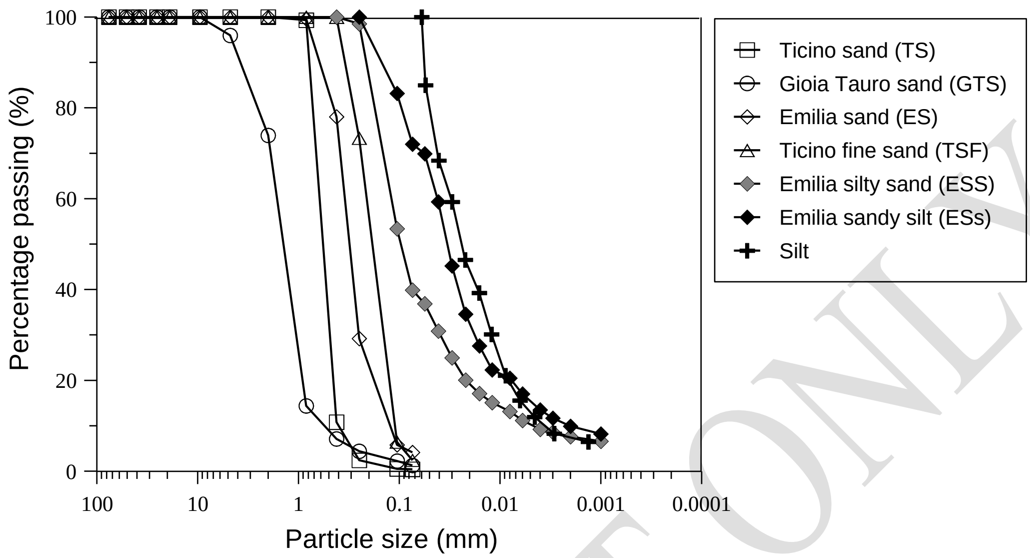

Fig. 1 – Grain size-distribution curves of tested materials

Sand specimen prepared by air pluviation method was deposited through a funnel in air. During pluviation, the funnel was traversed laterally to maintain an approximately levelled surface of the deposit. After filling the cavity, the excess sand over the final grade was siphoned off by applying a small vacuum. Samples prepared by the above pluviation methods were in the loosest state. Higher initial densities, when required, were obtained by tapping the base of the apparatus while the specimen was confined under a small seating load. When preparing *SS* specimens by water sedimentation method, the sand was spooned gently into the water layer by layer, until the height was just above the top of the mould. In this way, density index values D_r= 35-40% were initially achieved, regardless of the drop height. Higher densities were obtained by “tapping” on the lateral surface of the mould while maintaining a small seating load on the sample cap and keeping drainage lines open. When preparing *SS* specimens by moist tamping method, the under-compaction technique (Ladd 1978) of wet soil in two layers was used. Water content was calculated in order to achieve a degree of saturation equal to 50%**.** Due to the limited height of the specimen (only 2cm), the effects of inhomogeneity along its height can be neglected. It is worth mentioning that *CSS* tests were stopped when shear strains in single amplitude (γ_{SA}) reached 3.75%, which was assumed as liquefaction "triggering" criterion in all tests as recommended by several authors (Seed et al. 2003; Wu et al. 2004). Therefore, in the present study, N_f represents the number of cycles necessary to reach 3.75% shear strains (in single amplitude) under applied shear stress. The test program comprised 72 cyclic simple shear (*CSS*) tests; some additional cyclic triaxial tests carried out on undisturbed frozen sand samples of Gioia Tauro sand in previous research (Ghionna and Porcino 2006) was compared with that exhibited by the corresponding reconstituted *TX* specimens of the same sand. As far as cyclic triaxial tests are concerned, more details about apparatus and test procedure are reported in Ghionna and Porcino (2006). A summary of the testing program and initial test conditions are reported in Table 2.

Table 2 – Summary of the testing program

Soil type	Test type	Reconstitution method	e_0	D_r [%]	σ'_{vo} [kPa]	CSR	Tests
GTS	CTX	UNDIST.(frozen)/ WS	0.58 - 0.60	36 - 45	40	0.17 - 0.46	10
TS	CSS	AP / MT / WS	0.61 - 0.78	37 - 83	100	0.10 - 0.25	29
ES	CSS	WS	0.68 - 0.68	62 - 65	100	0.13 - 0.25	4
TSF	CSS	AP / WS	0.73 - 0.76	58 - 67	100	0.12 - 0.18	7
TS+5%Silt	CSS	MT	0.68	52	100	0.14 - 0.20	3
TS+10%Silt	CSS	MT	0.68	38	100	0.10 - 0.16	4
TS+20%Silt	CSS	MT	0.68	26	100	0.10 - 0.12	3
TS+30%Silt	CSS	MT	0.68	28	100	0.08 - 0.14	4
TS+35%Silt	CSS	MT	0.68	39	100	0.10	1
TS+40%Silt	CSS	MT	0.68	56	100	0.10 - 0.16	4
ESS	CSS	UNDIST.	0.53 - 0.84	-	130 - 150	0.17 - 0.26	9
ESs	CSS	UNDIST.	0.67 - 1.10	-	100	0.17 - 0.25	4

3. Prediction of cyclic pore water pressure (PWP) in clean sands by the damage-based concept

Pore water pressure model based on damage parameter requires a proper selection of the calibration parameters (CSR_t, α, β) (from Equations 3 to 6). Test results were initially analyzed to verify the dependence of the empirical parameter β of the modified Seed's pore pressure model (Eq. 4) from initial fabric induced by sand reconstitution method (i.e. moist tamped, air pluviation and water sedimentation). In fact, such an aspect was not throughly investigated in previous research and needs further verifications (Cetin and Bilge 2012). Figure 2 reports experimental data in $R_{u,res}$ versus D/D_f domain and, for comparison purposes, the upper and lower bounds suggested for clean sands by Seed et al. (1975), corresponding to β values ranging from 0.6 to 1.0.

Plots in Figure 2 reveal that pore water pressure generated in undrained *CSS* tests performed at various cyclic stress ratios ($CSR=\tau_{cyc}/\sigma'_{v0}$) and relative densities, can be well interpolated by Eq. (4) indicating a monotonically increasing function of the pore water pressure with a normalized damage parameter. The original boundary curves of pore-water pressure generation proposed by Seed et al. (1975) cannot, however, encapsulate all the data points because the suggested upper limit (β=1) does not serve as an upper cap for the observed PWP response. This is clearly evident for sand specimens reconstituted by water sedimentation method (Figure 2c).

The values of β empirical parameter (lower, upper, and best-fit), are reported in Table 3 for all tested sands and sample preparation methods.

Accordingly, β values corresponding to the lower and upper boundary curves of Seed's model should be revised also taking into account the strong influence exercised by the initial fabric of natural soil deposits.

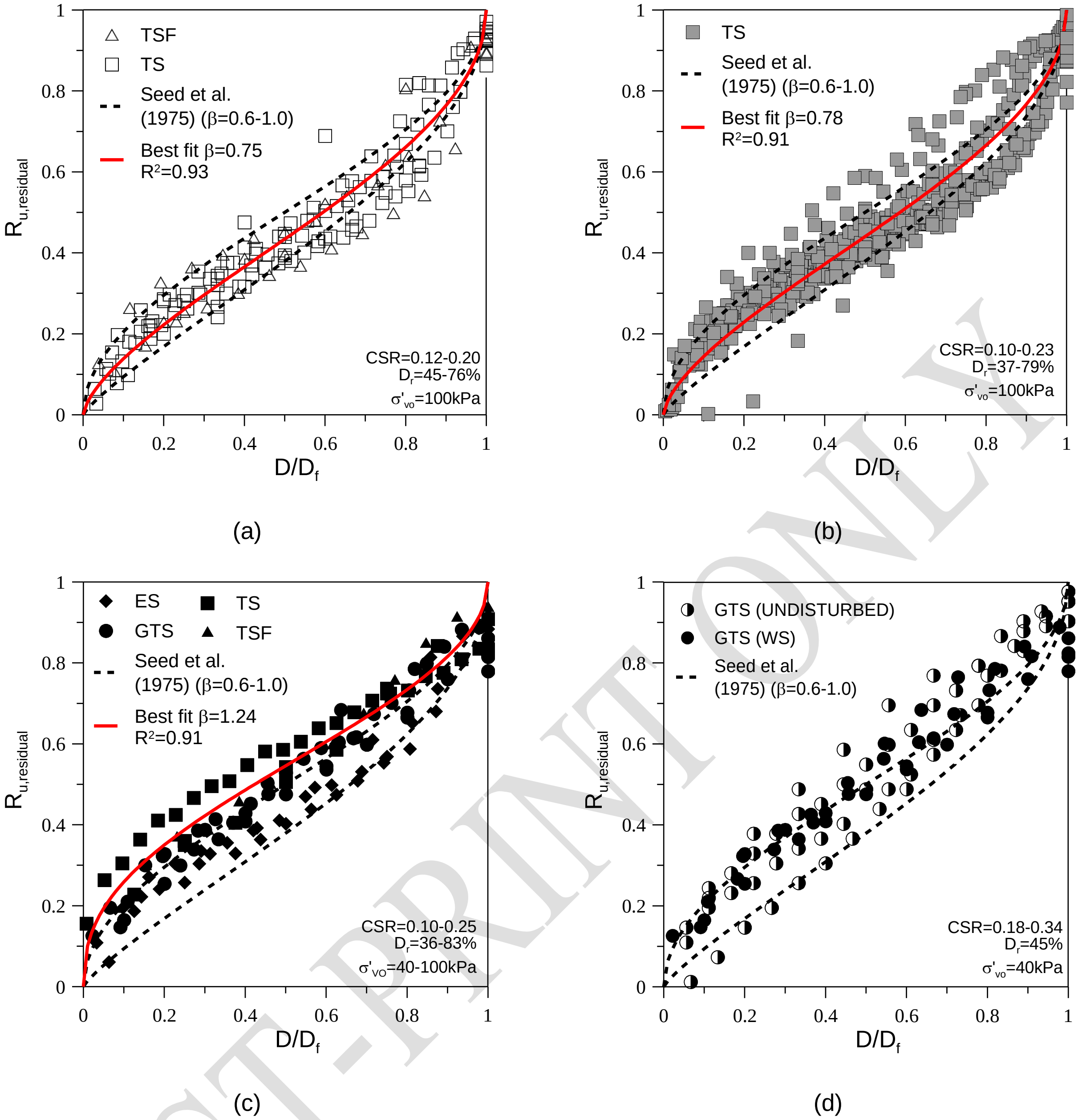

Fig. 2 – Comparison of test results with Seed et al. (1975) boundary curves for clean sands: a) air pluviation (AP); b) moist tamping (MT); c) water sedimentation (WS) and d) undirsturbed (in-situ frozen) samples.

Table 3 – Empirical parameter β (Equ. 4) for clean sands tested at several reconstitution methods

Sample Preparation method	**Sand**	$\beta_{lower/upper}$	$\beta_{best\ fit}$	R^2
AP	TS/TSF	0.53 – 1.29	0.75	0.93
MT	TS	0.50 – 1.50	0.78	0.91
WS	TS/GTS/TSF/ES	0.70 – 1.55	1.24	0.91
UNDISTURBED (frozen)	GTS	0.69 – 1.60	0.99	0.90

This aspect can also explain to some extent the discrepancies observed between β values gathered in the present research from clean sands and those recommended by Polito et al. (2008) through Eq. (2) for *FC*=0.

Experimental best fit β for clean sands reconstituted by *WS* are higher than those estimated from Eq. (2), whereas the predicted and measured values are quite similar to each other for sands prepared by moist-tamping, which was precisely the method adopted by Polito et al. (2008) .

Previous laboratory studies performed by the authors (Porcino and Marcianò 2008) demonstrated that modeling water deposited in-situ sands, such as those formed by the marine water environment, or fluvial soils, by their WS equivalent may be appropriate if the sands are uncemented and unaged.

A direct comparison of the cyclic pore water pressure pattern for *WS* and undisturbed samples of Gioia Tauro sand recovered by in-situ ground freezing (Ghionna and Porcino 2006) (Figure 2d and Table 3), supports such evidence.

A correlation relating β to relative density (D_r), cyclic stress ratio (*CSR*), mean grain size (D_{50}) and fines content (*FC*) for clean sands is presented through the following general mathematical form:

$$\beta = \mathrm{a} + \mathrm{b} \cdot \mathrm{FC} + \mathrm{c} \cdot \mathrm{D_r} + \mathrm{d} \cdot \mathrm{CSR} + \mathrm{e} \cdot D_{50} \qquad (7)$$

where *a*, *b*, *c, d* and *e* are regression constants (dimensionless), D_r and *FC* are expressed in percent.

To account for the effect of initial fabric, different regression coefficients resulted from analysis of tests carried out by *AP*, *WS* and *MT* sand preparation methods. Except for *AP*, the correlation coefficient R^2 values of the regressions were found to be greater than 0.70, so that the predictability is expected to be acceptable.

In particular, for moist tamping (R^2= 0.78), Eq.(7) may be re-written as:

$$\beta = -0.18281 + 0.00802 \cdot \mathrm{D_r} + 3.8322 \cdot \mathrm{CSR} \tag{8}$$

For water sedimentation (R^2= 0.70):

$$\beta = 1.67909 - 0.15238 \cdot \mathrm{FC} + 0.0013 \cdot \mathrm{D_r} - 1.50202 \cdot \mathrm{CSR} - 0.18186 \cdot \mathrm{d_{50}} \tag{9}$$

The pore water pressure model based on the concept of damage parameter cannot be used in default of measured CSR-N_f curves. The suggested procedure to derive calibration parameters (CSR_t, α) was based on cyclic *SS* test results, considering that the stress path imposed by a simple shear test better represents actual soil response under vertically propagating shear waves. The procedure was verified for a wide range of sands with different grain-sizes, relative densities and initial fabrics. The calculated calibration parameters, CSR_t and α*,* are listed in Table 4 for all clean sands tested in the present paper.

Table 4 – Empirical damage parameters recommended for clean sands tested in the present study

Material	**Specimen**	**α**			**CSR_t**			**CSR_{ref}**			**R^2**		
		L	**M**	**D**	**L**	**M**	**D**	**L**	**M**	**D**	**L**	**M**	**D**
GTS	WS	1.228	-	-	0.175	-	-	0.229	-	-	0.99	-	-
GTS	UND	0.989	-	-	0.184	-	-	0.215	-	-	0.99	-	-
TS	AP	2.490	2.684	2.577	0.064	0.079	0.070	0.110	0.127	0.152	0.98	0.96	0.99
TS	MT	2.080	2.517	2.730	0.097	0.093	0.119	0.154	0.168	0.211	0.99	0.94	0.98
TS	WS	2.080	-	-	0.062	-	-	0.133	-	-	0.99	-	-
TSF	AP	-	2.850	-	-	0.072	-	-	0.133	-	-	0.98	-
ES	WS	-	2.950	-	-	0.077	-	-	0.157	-	-	0.92	-
TSF	WS	-	2.430	-	-	0.049	-	-	0.139	-	-	0.98	-

Note:
L = loose (relative densities range from 36 to 45 %)
M = medium dense (relative densities range from 62 to 66 %)
D = dense (relative densities range from 75 to 83%)

Figure 3a reports experimental data of clean Ticino sand prepared at various density states from cyclic *SS* tests, together with the corresponding CSR-N_f curves calculated from the model based on damage parameter (Eq. 6).

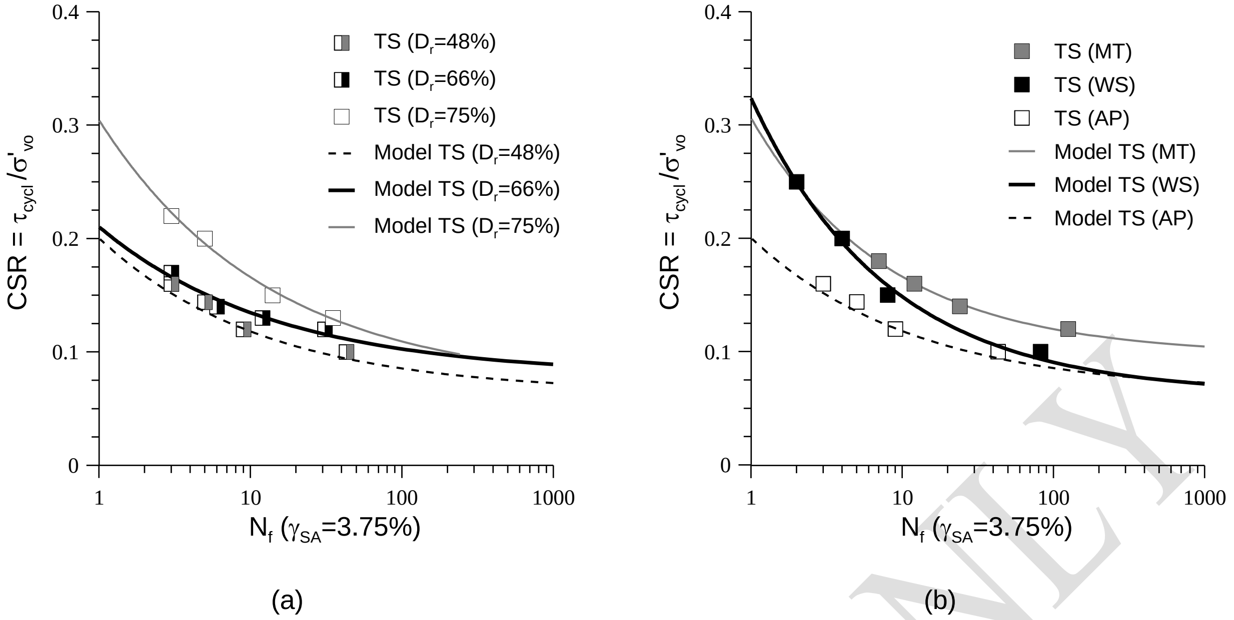

Fig. 3 – Liquefaction resistance curves obtained by damage-based model for Ticino sand tested at: a) different relative densities (AP) b) different reconstitution methods (loose).

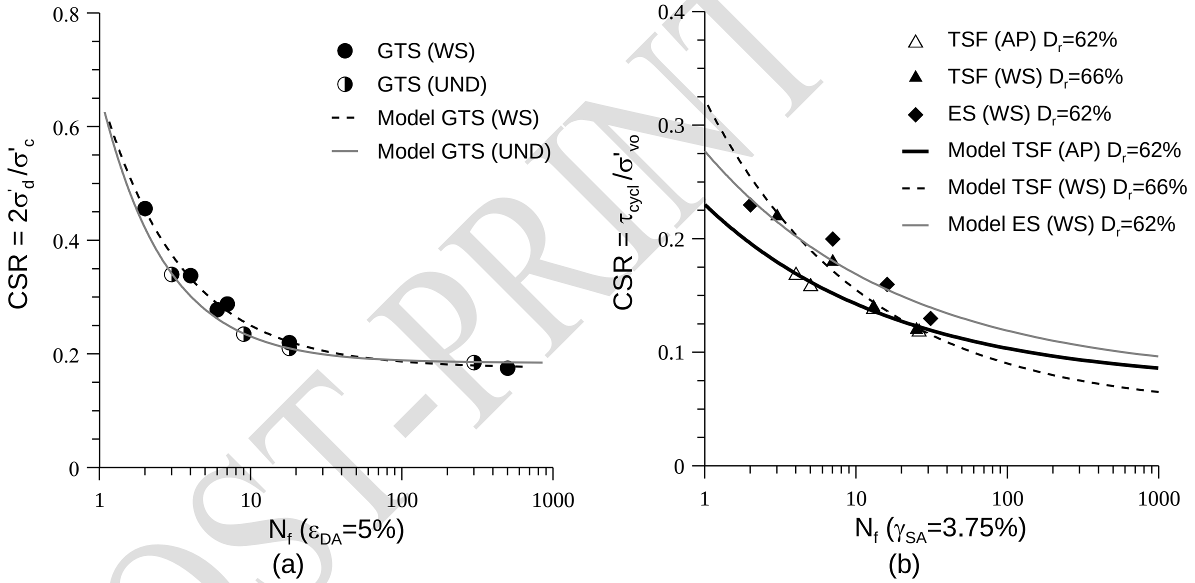

Fig. 4 – Liquefaction resistance curves calculated by damage-based model for clean sands: a) Gioia Tauro coarse sands, b) fine sands.

For all cyclic resistance curves, CSR_t was selected as the value corresponding to a high number of loading cycles (i.e. 500) in experimental CSR-N_f curve; in any case, Figures 3 and 4 evidence that the curves constructed by the suggested methodology match the experimental data points well, regardless of grain size of tested sand and adopted sample preparation method (R^2 values greater than 0.92). It is worth mentioning that the accuracy in the prediction of the model, evaluated through comparisons with measured data, can be improved if data points at large number of cycles are also available (see Figures 3b and 4a). In particular, for loose to medium dense sands with 0.18mm≤D_{50}≤0.56mm the resulting α values (ranging from 2.080 to 2.95) and CSR_t values (ranging from 0.049 to 0.097) lie in a narrow band for different initial fabrics (Table 4).

As previously outlined, the class of so-called "damage parameter models" cannot be used in the absence of measured CSR-N_f curve. Figure 5 reports the range of normalized resistance curves against liquefaction (where *CSR* was normalized *by* $CSR_{N=15}$.) including all data points of clean sands tested in the present study. The CSR-N_f relations, shown in Figure 5, are nearly linear on a log-log plot and a band of normalized results from these simple shear tests is reported for different sample preparation methods. As can be argued, the band of the normalized recommended curves depends on the relative density, and intrinsic factors such as gradation/angularity of sand.

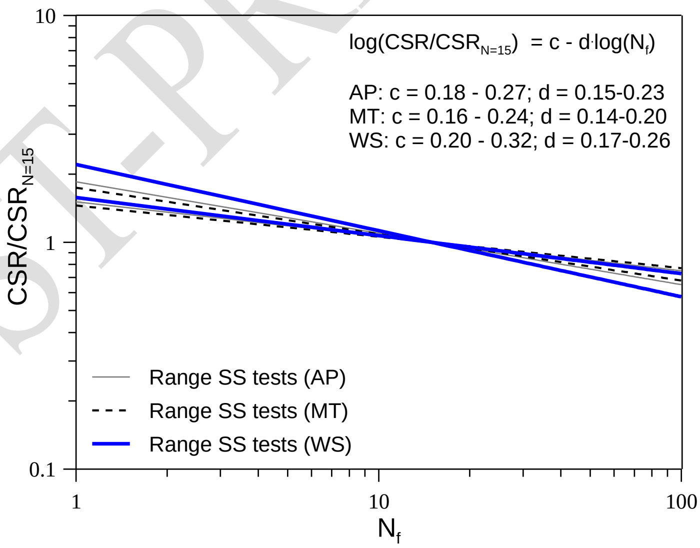

Fig. 5 – Normalized cyclic liquefaction resistance curves to be used for pore pressure prediction by "stress-based" models.

In order to investigate the correspondence between "stress and strain controlled tests", the upper and lower boundaries proposed by Dobry (1985) on the basis of strain-controlled cyclic tests, are given in Figure 6, in the $R_{u,res}$ vs. γ_{max} domain.

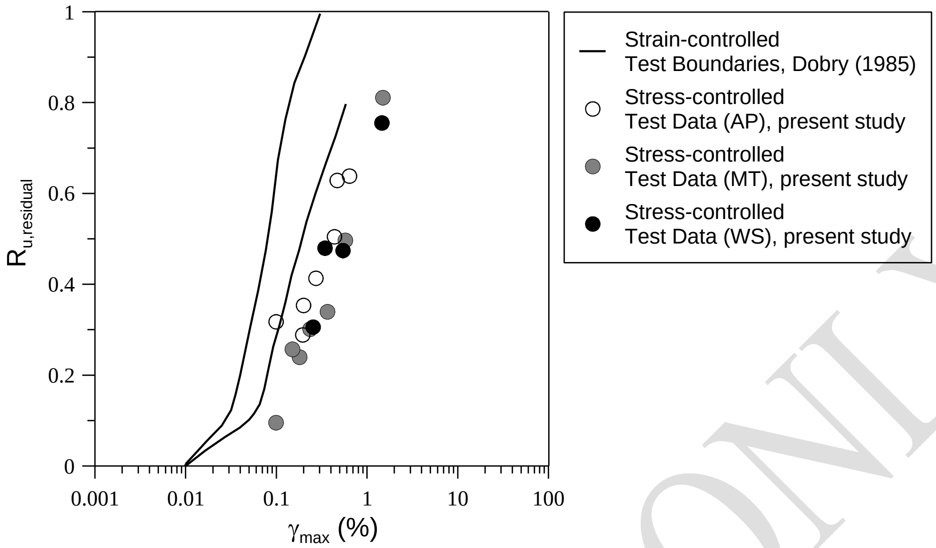

Fig. 6 – Comparison of experimental test results with Dobry (1985) boundary curves.

In the same plot, experimental data gathered from stress-controlled *CSS* tests performed on clean sands in the present study, are also superimposed. In particular, the data refer to $R_{u,res}$ values measured after 10 cycles of applied shear stress (stress-controlled) or applied shear strains (strain-controlled) and γ_{max} is the maximum double-amplitude cyclic shear strain. Even though strain paths followed during the two test types are different, the experimental data are very close to the lower boundary suggested by Dobry (1985) (Figure 6). Additionally, a unique relation $R_{u,res}$ vs. γ_{max} can be tentatively attempted, regardless of sample reconstitution method.

4. Prediction of cyclic pore water pressure (PWP) in silty sands by the damage-based concept

In the present section, data from stress-controlled *CSS* tests carried out on silty sands to sandy silts were analyzed for modeling purposes. A plot of the residual excess pore pressure build-up for Ticino sand + silt mixtures (e_0=0.68) with respect to the normalized damage parameter is given in Figure 7a. As may be seen, even for sands with non-plastic fines less than 35%, Eq. (4) can still successfully be applied for predicting pore water pressure under cyclic loading based on damage parameter.

Also displayed in Figure 7a are the upper and lower bounds of measured residual R_u according to Eq. (4) for silty sands (*FC*<35%). The values of β obtained by regression analysis for various fines contents are listed in Table 5 (best-fit).

Although some scatter is observed, there is a clear dependence of the model parameter β on fines content (Figure 8a), in agreement with the findings suggested by other authors (i.e. Polito et al. 2008) on the basis of cyclic TX tests conducted on sand-silt mixtures (*FC*<35); however, the experimental β values are generally higher than those predicted from the Polito's relationship, regardless of percentage of fines.

Table 5 – Empirical damage parameters recommended for silty sands (FC ≤35%) and β best-fit values of Seed et al. (1975) (Eq. 4)

Material	**Specimen**	α			**CSR$_t$**			**CSR$_{ref}$**			**R^2**	$\beta_{best\ fit}$	**R^2**
		L	**M**	**D**	**L**	**M**	**D**	**L**	**M**	**D**			
TS	MT	-	2.517	-	-	0.093	-	-	0.168	-	0.94	0.77	0.91
TS+5%Silt	MT	-	3.315	-	-	0.081	-	-	0.160	-	0.86	0.78	0.93
TS+10%Silt	MT	2.580	-	-	0.065	-	-	0.128	-	-	0.98	1.06	0.93
TS+20%Silt	MT	2.370	-	-	0.052	-	-	0.105	-	-	0.99	0.84	0.94
TS+30%Silt	MT	2.390	-	-	0.046	-	-	0.100	-	-	0.99	1.15	0.97

Note: Tests performed at a constant (globalo) void ratio e_0=0.68

L = loose (relative densities range from 26 to 39 %)

M = medium dense (relative densities range from 52 to 65 %)

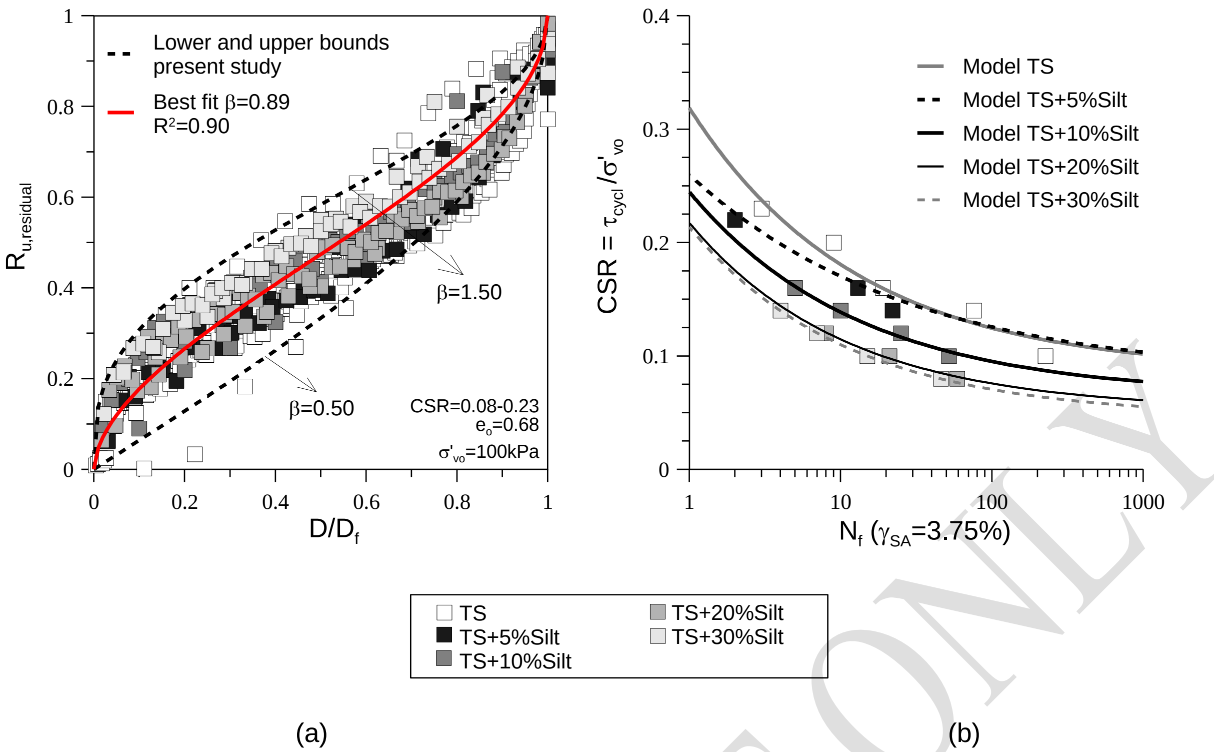

Fig. 7 – Comparison of: (a) measured data and predicted pore pressure; b) measured and predicted CSR-N_f curves for silty sands (FC ≤35%).

The role of non-plastic fines on liquefaction susceptibility of silty sands is apparent from Figure 7b, where cyclic stress ratios are plotted against the corresponding number of loading cycles to initial liquefaction. It is worth noticing that, when the comparison is made at a constant (global) void ratio value, an increase of non-plastic fines entails a decrease of a cyclic shear strength until a limiting fines content (*LFC*) is achieved. This value of *LFC* was estimated to be 30% for the tested sand-silt mixtures.Figure 7b also compares the predicted CSR-N_f curves with the experimental data. It is evident that the recommended procedure for selecting model calibration parameters (CSR_t, α) (Table 5 and Figure 7b) provides an accurate prediction of cyclic liquefaction resistance curves also for sand-silt mixtures (R^2>0.86), with values of CSR_t ranging from 0.046 to 0.093 and α ranging from about 2.3 to 3.3. It should be noted that the Seed et al. model has its limitations when applied to sands with a fines content higher than 35%, since the pattern of PWP response changes for sands having *FC* less than and greater than 35% (see Figures 9a and 9b).

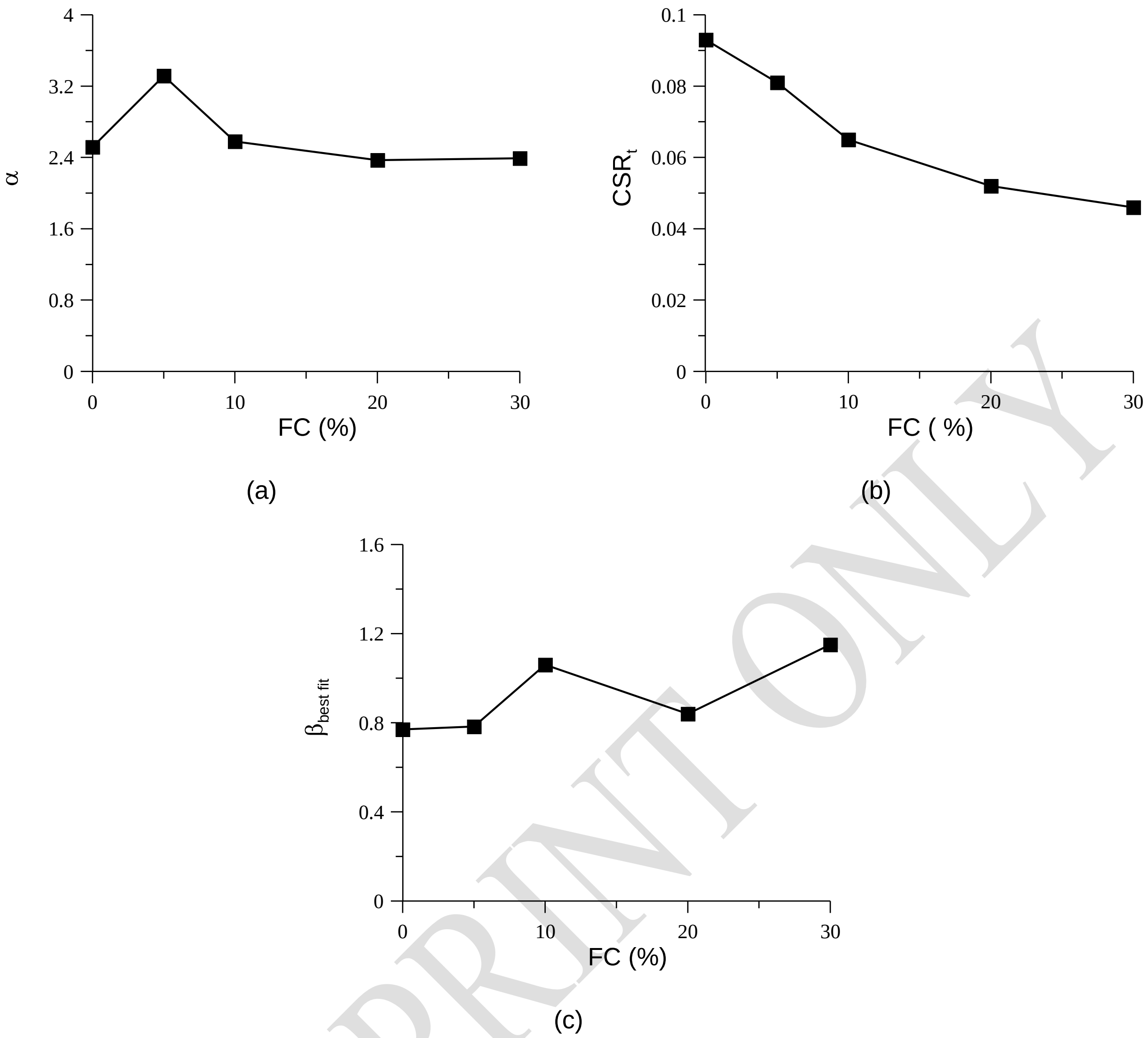

Fig. 8 - Variation of the parameters α, CSR_t and $\beta_{best\ fit}$ with fines content for silty sands at a (global) void ratio e_0=0.68.

It is not altogether surprising, as it is consistent with the limiting silt content concept (Polito 1999; Polito and Martin 2001; Green et al. 2006). For this reason, in the present study for soils with *FC*>35%, a new simple relationship between the residual pore water pressure ratio and the damage parameter was proposed:

$$R_{u,res} = a \cdot \left(\frac{D}{D_f}\right)^b \tag{10}$$

where *a* and *b* are the two parameters controlling the shape of the curve, obtained from the best fitting through the available *CSS* laboratory results.

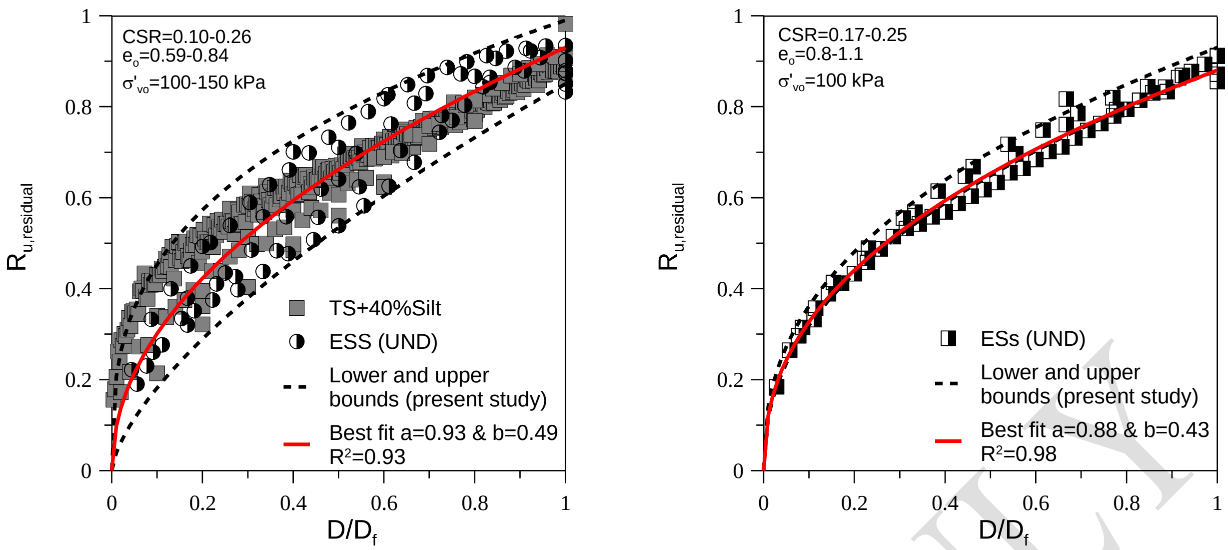

(a) (b)

Fig. 9 – Pore water pressure ratio vs. normalized damage parameter for silty soils and application of the new model proposed in the present study for *FC*>35% (Eq. 10).

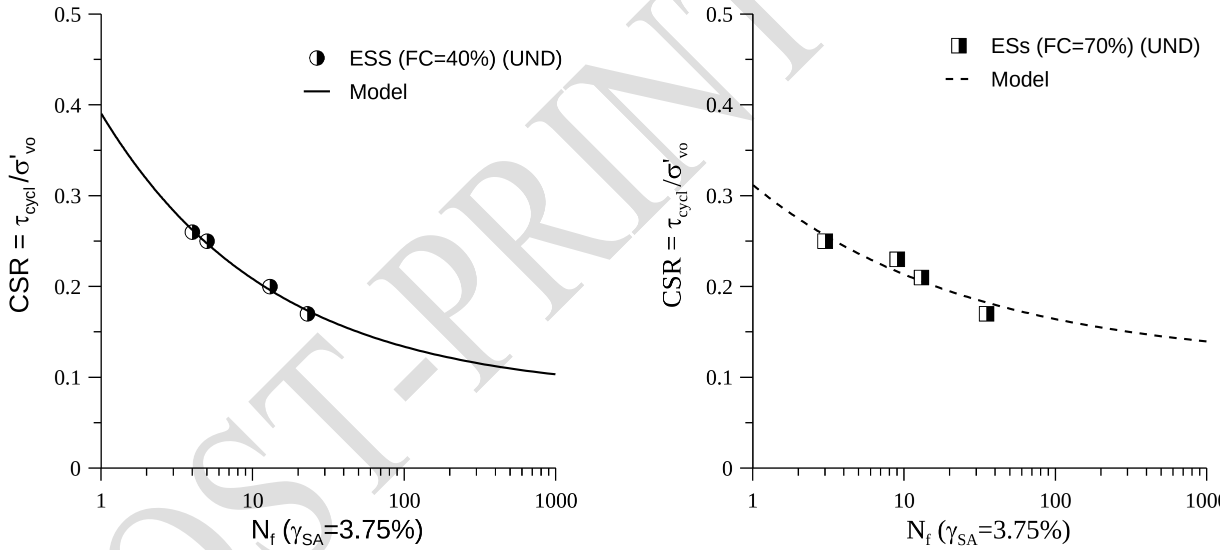

(a) (b)

Fig. 10 – Cyclic resistance curves calculated by the new damage-based model for Emilia silty soils.

An application of the new simple relationship for predicting excess pore water pressure rise during cyclic loading has been presented in Figures 9(a) and 9(b) for Emilia undisturbed samples (ESS and ESs) recovered after the 2012 earthquake, in Italy. It may be argued that Eq. (10) fits data points with greater overall accuracy and, therefore, it is suitable for soils with FC>35%.

Definitively, the revised damage-based model through Equations (3), (5), (6) and (10) is capable of interpreting the measured CSR-N_f data (Figure 10) and predicting the experimental pore water pressure generation (Figure 9) of low plasticity silty materials having 40%<*FC*<70% very well.

All parameters necessary for the assessment of normalized damage parameter are reported in Table 6 for the tested soils.

Table 6 – Empirical damage parameters recommended for sands with FC>35% and empirical parameters *a* & *b* of Eq. (10)

Material	Specimen	α	CSR_t	CSR_{ref}	R^2	$a_{best\ fit}$	$b_{best\ fit}$	R^2
TS+40%Silt	MT	2.193	0.093	0.133	0.99	0.86	0.35	0.95
ESS - FC=40%	Undisturbed	2.557	0.082	0.190	0.99	0.93	0.49	0.93
ESs - FC=70%	Undisturbed	3.315	0.115	0.202	0.89	0.88	0.43	0.98

The pore water pressure model based on damage parameter and accumulated stress is nowadays implemented in DEEPSOIL seismic analysis code (Hashash et al. 2016) and the applicability of the model was validated for sandy soils through comparisons with laboratory data mostly of which came from cyclic triaxial tests (Park and Ahn 2013; Park et al. 2015).

However, definitive conclusions on the proper choice of calibration parameters and the limitations of the suggested procedure require more systematic investigation, as discussed in depth in the present research.

In order to verify the generality of the new procedure based on the proposed relationship for R_u=F(D/D_f) (Eq. 10) in the case of low plasticity silty sandy soils (FC>35%), some decoupled analyses were carried out for the irregular stress histories by the 2012 Emilia earthquake in Italy (M_w=6.1), shown in Figure 11. Since no acceleration records were available at the site of Scortichino, the procedures adopted for selection and scaling the input ground motion are reported in previous studies (Tonni et al., 2015). Only one reference input motion was adopted in the following analysis for simplicity (Fig. 11b). Soil deposits constitute a river bank at the site of Scortichino, where significant evidences of soil deformation and building damages were observed after the main seismic event (Tonni et al. 2015).

Figure 11a shows the soil profile and the related shear wave velocity profile obtained from borehole logs and geophysical tests, respectively. The normalized shear modulus and damping ratio curves, obtained from resonant column and cyclic simple shear tests (Tonni et al., 2015) are also shown in Figure 11c.

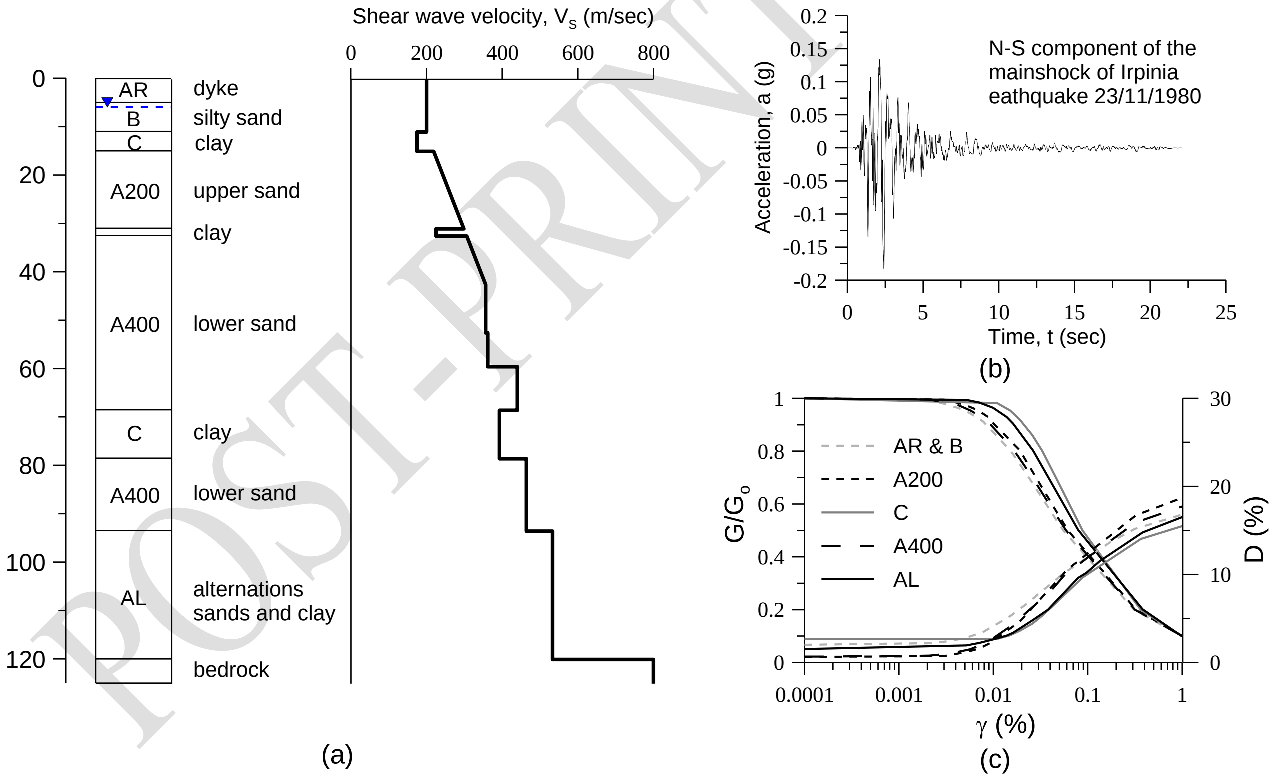

Fig. 11 – Soil profile and Vs profile (a),reference input motion (b); variation of the normalized shear modulus and damping with the shear strain (γ) (c).

In the decoupled approach, the shear stress-time history, as computed at specific depths by a total stress seismic response analysis (DEEPSOIL), was then transformed to values of the damage parameter *D* and the magnitude of pore water pressure was determined directly from Eq. (10).

The pore water pressure resulting from the application of the new analytical function through Eq. (10) at 7 m depth, i.e. in the silty sand, was applied by using *a* and *b* parameters selected from Table 6 for soils with *FC*=40%. Pore water pressure history is given by the curve labeled “New Model” (Figure 12) and, for comparison purposes, the pore water pressure prediction computed by Eq. (4), associated with Polito et al. correlation for (Eq. 2), was plotted in the same Figure.

Marked differences can be found in PWP responses since the application of Eq. (4) leads to an apparent underestimation of PWP response if compared with the “New model”. This implies that the formulation of damage-based models should be modified to account for the effect of high fines contents when it is implemented in a seismic site analysis.

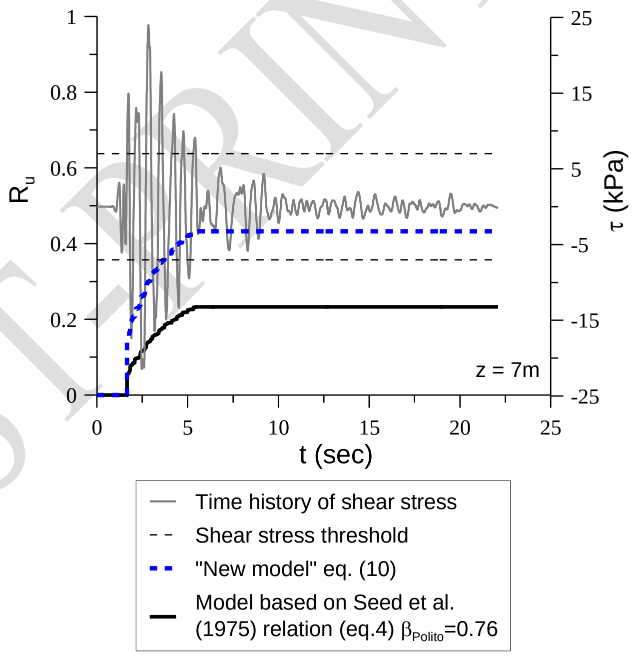

Fig. 12 – Shear stress and excess pore pressure ratio histories for Emilia silty sands (FC=40%) and application of the new relationship (Eq. 10) suggested in the present study.

Conclusions

In the present study, following the work developed by Park and Ahn (2013) and Park et al. (2015), an extensive experimental investigation was carried out on four clean sands, and silty soils of very low plasticity (both FC<35% and FC>35%) in order to predict the accumulation of pore water pressure build up to the initial liquefaction under irregular loading through the results of undrained simple shear tests. Pore water pressure was simply expressed as a monotonically increasing function of a single variable called "Damage parameter", which requires for its determination only CSR-N_f data from high quality cyclic undrained tests. A suitable and simple link between laboratory and field behaviour may be provided through the use of such a damage concept, since there is no longer any need to run additional analysis to convert the irregular stress history to equivalent uniform loading cycles before using data from laboratory tests. However, the tests for determining model parameters and the procedure followed for deriving them require considerable care and consideration of the main factors affecting PWP response of sandy soils. The main conclusions which can be drawn by the present study are the following:

- The pore water pressure model based on damage parameter for sands with FC<35% requires a proper selection of the calibration parameters (CSR_t, α, β) (Equations 3-6) which can be derived from undrained cyclic SS tests in a satisfactory way. The recommended parameters of the model (CSRt, α, β) can be properly selected in effective stress analysis, taking into account the influence of several factors such as: density state, grain size, sample preparation method and fines content.
- For FC>35%, modification to R_u=f(D/D_f) relationship is needed for estimating pore water pressure build-up in an accurate way. In this case, the proposed relationship between R_u and (D/D_f) ratio (Eq. 10) is defined as the best fitting function of the

available laboratory results carried out on undisturbed silty specimens, and it requires only two empirical parameters to be defined. The obtained empirical values for the two parameters of the proposed model lie in a narrow range for tested soils.

References

ASTM D4253 (2000) Standard Test Methods for Maximum Index Density and Unit Weight of Soils Using a Vibratory Table. ASTM international, West Conshohocken,PA, pp 1-14

ASTM D4254 (2000) Standard Test Methods for Minimum Index Density and Unit Weight of and Calculation of Relative Density. ASTM international, West Conshohocken,PA, pp 1-9

Baziar MH, Shahnazari H Sharafi H (2011) A laboratory study on the pore pressure generation model for Firouzkooh silty sands using hollow torsional test. International J Civ Eng 9 (2): 126-134

Belkhatir M, Schanz T, Arab A, Della N (2014) Experimental study on the power water pressure generation characteristics of saturated silty sands. Arab J Sci Eng 39(8):6055–6067

Berrill JB, Davis RO (1985) Energy Dissipation and Seismic Liquefaction of Sands: Revised Model. Soils Found 25(2):106-118

Booker JR, Rahman MS, Seed HB (1976) GADFLEA–a computer program for the analysis of pore pressure generation and dissipation during cyclic of earthquake loading. Earthq Eng Cent, University of California at Berkeley, Berkeley, CA

Bryne PM (1991) A Cyclic Shear-Volume Coupling and Pore Pressure Model for Sand. In: Proc Second Int Conference on Recent Advances in Geotech Earthq Eng and Soil Dyn, St. Louis, Missouri, pp 47-55

Burghignoli A, Pane V, Sagaseta C, Cuellar V, Pastor M (1991) Modelling stress–strain-time behaviour of natural soils. In: Proc of the 10th European conference on soil mechanics and found eng, Florence, vol. 3, pp 959–99

Cetin KO, Bilge HT (2011) Cyclic large strain and induced pore pressure models for saturated clean sands. J Geotech Geoenviron Eng 138(3): 309-323. doi:10.1061/(ASCE)GT.1943-5606.0000631

Chang CS, Kuo CL, Selig ET (1981) Pore pressure development during cyclic loading. J Geotech Eng 109(1):103–107

Chang WJ (2002) Development of an in situ dynamic liquefaction test. Dissertation, University of Texas at Austin

Chang WJ, Rathje EM, Stokoe KH, Hazirbaba K (2007) In situ pore-pressure generation behavior of liquefiable sand. J Geotech Geoenviron Eng 133(8): 921-931. doi:10.1061/(ASCE)1090-0241(2007)133:8(921)

Chiaradonna A, Tropeano G, d'Onofrio A, Silvestri F, Park D (2015) Application of a simplified model for the prediction of pore pressure build-up in sandy soils subjected to seismic loading. In: Proc 6th International Conference Earthq Geotech Eng, Christchurch, New Zealand.

Dash HK, Sitharam TG (2009) Undrained cyclic pore pressure response of sand-silt mixtures: effect of nonplastic fines and other parameters. J Geotech Geolog Eng 27(4): 501-517. doi:10.1007/s10706-009-9252-5

Davis RO, Berrill JB (2001) Pore pressure and dissipated energy in earthquakes—Field verification. J Geotech Geoenviron Eng 127(3): 269–274. doi:10.1061/(ASCE)1090-0241(2001)127:3(269)

Derakhshandi M, Rathje EM, Hazirbaba K, Mirhosseini SM (2008) The effect of plastic fines on the pore pressure generation characteristics of saturated sands. Soil Dyn Earthq Eng 28(5): 376–386. doi:10.1016/j.soildyn.2007.07.002

Dobry R (1985) Liquefaction of soils during earthquakes. Rep No. CETS-EE-001, Natl Res Council (NRC), Committee on Earthq Eng, Washington, DC

Dobry R, Ladd R, Yokel F, Chung R, Powell D (1982) Prediction of pore water pressure buildup and liquefaction of sands during earthquakes by the cyclic strain method. Natl Bur Stand build science ser 138, Gaithersburg

Dobry R, Pierce WG, Dyvik R, Thomas GE, Ladd RS (1985) Pore pressure model for cyclic straining of sand. Res Rep 1985-06, Rensselaer Polytechnic Institute, Troy, NY

Dyvik R, Berre T, Lacasse S, Raadim B (1987) Comparision of truly undrained and costant volume direct simple shear tests. Geotechnique 37(1): 3-10. doi: 10.1680/geot.1987.37.1.3

Figueroa J, Saada AS, Liang L, Dahisaria NM (1994) Evaluation of Soil Liquefaction by Energy Principles. J Geotech Eng 120(9):1554-1569. doi:10.1061/(ASCE)0733-9410(1994)120:9(1554)

Finn WDL (1985) Aspects of constant volume cyclic simple shear. In: Proc Advances in the art of testing soils under cyclic conditions, ASCE New York, pp 74–98

Finn WDL, Bathia SK (1982) Prediction of seismic pore water pressures. In: 10th International conference in soil mechanics and found, Stockholm, pp 201-206

Ghionna VN, Porcino D (2006) Liquefaction resistance of undisturbed and reconstituted samples of a natural coarse sand from undrained cyclic triaxial tests. J Geotech Geoenviron Eng 132(2):194-202. doi:10.1061/(ASCE)1090-0241(2006)132:2(194)

Green RA (2001) Energy-based evaluation and remediation of liquefable soils. Dissertation, Virginia Polytechnic Institute and State University

Green RA, Mitchell JK, Polito CP (2000) An energy-based excess pore-water pressure generation model for cohesionless soils. In: Proc Developments in Theoretical Geomechanics-The John Booker Memorial Symposium ,Sydney, New South Wales, Australia, pp 16-17

Green RA, Olson SM, Polito CP (2006) A comparative study of the influence of fines on the liquefaction susceptibility of sands: Field versus laboratory. In: Proc 8th National Conference on Earthq Eng, Earthq Eng Res Inst, Oakland, CA

Hashash YMA, Musgrove MI, Harmon JA, Groholski DR, Phillips CA, Park D (2016) DEEPSOIL 6.1, User Manual. Urbana, IL, Board of Trustees of University of Illinois at Urbana-Champaign

Hashash YMA, Phillips C, Groholski DR (2010) Recent Advances in non-linear site response analysis. In: 15th International Conference on Recent Advances in Goetech Earthq Eng and Soil Dyn, San Diego, CA

Hazirbaba, K (2005) Pore pressure generation characteristics of sands and silty sands: a strain approach. Dissertation, University of Texas at Austin

Hazirbaba K, Rathje EM (2004) A comparison between in situ and laboratory measurements of pore water pressure generation. In: Proc 13th World Conference on Earthq Eng, Vancouver, Canada.

Ishihara K, Lysmer J, Yasuda S, Hirao H (1976) Prediction of liquefaction in sand deposits during earthquakes. Soils and Found 16(1):1-16. doi:10.3208/sandf1972.16.1

Ivši´c T (2006) A model for presentation of seismic pore water pressures. Soil Dyn Earthq Eng 26(2):191-199. doi:10.1016/j.soildyn.2004.11.025

Konstadinou M, Georgiannou VN (2014) Prediction of pore water pressure generation leading to liquefaction under torsional cyclic loading. Soils and Found 54(5): 993-1005. doi:10.1016/j.sandf.2014.09.010

Ladd RS (1978) Preparing test specimens using undercompaction. Geotech Test J 1(1): 16-23. doi:10.1520/GTJ10364J.

Lee KL, Albaisa A (1974) Earthquake induced settlements in saturated sands. J Geotech Eng Division 100(4): 387–405

Martin GR, Finn WDL, Seed HB (1975) Fundamentals of liquefaction under cyclic loading. J Geotech Eng Division 101(5):423–438

Matasovic N, Vucetic M (1993) Cyclic Characterization of Liquefiable Sands. J Geotech Geoenviron Eng 119(11): 1805-1822. doi:10.1061/(ASCE)0733-9410(1993)119:11(1805)

Mulilis PJ, Seed BH, Chan CK, Mitchell JK, Arulanandan K (1977) Effects of Sample Preparation on Sand Liquefaction. J Geotech Eng Division 103 (2): 91–108

Park T, Ahn JK (2013) Accumulated stress based model for prediction of residual pore pressure.In: Proc of the 18th International Conference on Soil Mechanics and Geotechl Eng, Paris, France

Park T, Park D, Ahn JK (2015) Pore pressure model based on accumulated stress. Bull Earthq Eng 13(7): 1913-1926. doi:10.1007/s10518-014-9702-1

Polito CP (1999) The effects of non-plastic and plastic fines on the liquefaction of sandy soils. Dissertation, Virginia Polytechnic Institute and State Univ, Blacksburg, VA

Polito CP, Green RA, Dillon E, Sohn C (2013) Effect of load shape on relationship between dissipated energy and residual excess pore pressure generation in cyclic triaxial tests. Canadian Geotech J 50(11):1118–1128. doi:10.1139/cgj-2012-0379

Polito CP, Green RA, Lee J (2008) Pore pressure generation models for sands and silty soils subjected to cyclic loading. J Geotech Geoenviron Eng 134(10):1490-1500. doi:10.1061/(ASCE)1090-0241(2008)134:10(1490)

Polito CP, Martin JR II (2001) Effects of non-plastic fines on the liquefaction resistance of sands. J Geotech Geoenviron Eng 127(5):408–415. doi:10.1061/(ASCE)1090-0241(2001)127:5(408)

Porcino D, Caridi G, Malara M, Morabito E (2006) An automated control system for undrained monotonic and cyclic simple shear tests. In: Proc Geotech Eng in the Information Technology Age, American Society of Civil Engineers, Reston, Va, pp 1-6

Porcino D, Diano V (2016) Laboratory Study on Pore Pressure Generation and

Liquefaction of Low-Plasticity Silty Sandy Soils during the 2012 Earthquake in Italy. J Geotech Geoenviron Eng 142(10): 04016048. doi:10.1061/(ASCE)GT.1943-5606.0001518

Porcino D, Marcianò V (2008) Effect of initial fabric on cyclic and monotonic undrained shear strength of Gioia Tauro sand. In: Proc of the 2008 Seismic Engineering Conference commemorating the 1908 Messina and Reggio Earthquake Part I, Reggio Calabria, pp 448-455

Rathje E, Chang W, Stokoe K (2005) Development of an In Situ Dynamic Liquefaction Test. Geotech Test J 28(1): 1-11. doi:10.1520/GTJ12289

Sagaseta C (1995) Soil properties and their measurement. In: Proc of Wroth memorial symposium—predictive soil mechanics. Thomas Telford London

Seed RB, Cetin KO, Moss RES, Kammerer A, Wu J, Pestana J, Riemer MF, Sancio RB, Bray JD, Kayen RE, Faris A (2003) Recent advances in soil liquefaction engineering: A unified and consistent framework. In: Keynote presentation, 26th Annual ASCE Los Angeles Geotechnical Spring Seminar, Long Beach, CA.

Seed HB, Idriss IM (1982) Ground motions and soil liquefaction during earthquakes. Earthquake, Eng Res Inst, Berkeley, Ca

Seed HB, Martin PP, Lysmer J (1975) The generation and dissipation of pore water pressures during soil liquefaction. Report No. UCB/EERC 75-26. Earthq Eng Center, University of Berkeley, CA

Seed HB, Pyke RM, Martin GR (1978) Effect of multi-directional shaking on pore-pressure development in sands. J Geotech Eng Division, 104(1): 27-44

Tonni L et al. (2015) Interpreting the deformation phenomena triggered by the 2012 Emilia seismic sequence on the Canale Diversivo di Burana banks (Analisi dei fenomeni deformativi indotti dalla sequenza emiliana del 2012 su un tratto di argine del Canale Diversivo di Burana (FE)). Italian J Geotech 46(2):28-58

Vucetic M (1994) Cyclic threshold shear strain in soils. J Geotech Eng,120(12): 2208-2228. doi:10.1061/(ASCE)0733-9410(1994)120:12(2208)

Wu J, Kammerer AM, Riemer MF, Seed RB, Pestana JM (2004) Laboratory study of liquefaction triggering criteria. In: 13th World Conference on Earthq Eng, Vancouver, BC, Canada, Paper (No. 2580)

Youd TL (1972) Compaction of sands by repeated shear straining. J Soil Mechanics and Found Division 98(7):709-725